ELSEVIER

Journal of Photochemistry and Photobiology A: Chemistry 141 (2001) 109–116

Journal of Photochemistry and Photobiology A:Chemistry

www.elsevier.nl/locate/jphotochem

Photophysical/quantum mechanical characterization of the compound 3-benzoxazol-2-il-7-hydroxy-chromen-2-one

Antonio Eduardo da Hora Machado*, Jacques Antonio de Miranda

Universidade Federal de Uberlândia, Instituto de Química, PO Box 593, 38400-089 Uberlândia, Minas Gerais, Brazil

Received 25 March 2001; received in revised form 17 April 2001; accepted 25 April 2001

Abstract

The photophysical properties of the compound 3-benzoxazol-2-il-7-hydroxy-chromen-2-one were studied for different solvents. This compound, due to a dissociation equilibrium based on the hydroxyl group, results in a neutral and an anionic form in protic solvents. Both forms present high molar absorptivities, around $10^4\,\mathrm{dm^3\,mol^{-1}\,cm^{-1}}$ related to the $S_0 \rightarrow S_1$ transition, which suggests for this transition a $\pi \rightarrow \pi^*$ character. Theoretical calculations show that this transition must possess some $n \rightarrow \pi^*$ perturbational contribution, principally in the case of the anionic form, where the dipole moment of the S_1 state (8.590 D) is lower than the observed for the ground state (9.374 D). For the neutral molecule, the $n \rightarrow \pi^*$ perturbational contribution is due to the ketonic group, whereas for the ionized form, this contribution is due to the phenoxide group. The theoretical prediction of the electronic spectra and microstates shows a good agreement with the experimental data, principally when the solvation is considered. This coumarin shows to be highly fluorescent in different solvents, presenting elevated quantum yields and large Stokes' shifts. The Stokes' shift for the neutral form, although the S_1 excited state present a higher dipole moment than the ground state, shows a trend to diminish as the solvent polarity increases, due to efficient solvent–fluorophore interactions in the ground state. The participation of non-radiative processes increases as the anionic form becomes preponderant and with the increase in the polarity of the solvent and its capacity to perform hydrogen bonding. Even at low temperature (77 K), phosphorescence was not detected. Meanwhile, a quantum yield of 0.06 for singlet oxygen generation was measured for the neutral species in chloroform, indicating the possibility of intersystem crossing in a low extent.

Keywords: Photophysics; Coumarin derivative

1. Introduction

Coumarins are a family of compounds that have been studied extensively due to its practical applications [1,2]. Optical brightners, laser dyes, sensitizers in phototherapy, etc., is some of the usefulness of this class of compounds (Fig. 1).

Electron-donor groups in the 4- and 7-position cause bathochromic and bathofluoric shifts, which are the larger, the more pronounced the electron-donor behaviour of the substituents [1,3,4]. Also, this kind of substitution and the increase in the solvent polarity are associated to the increase in the fluorescent properties of coumarins, due to inversion of states [4].

In this study, we evaluate some photophysical properties of the coumarin derivative 3-benzoxazol-2-il-7-hydroxy-chromen-2-one, and its anionic form (Scheme 1) comparing experimental and theoretical results.

2. Experimental

Dr. Ana Maria Ferreira de Oliveira-Campos, University of Minho, Portugal gently furnished the compound 3-benzoxazol-2-il-7-hydroxy-chromen-2-one. All the solvents were of spectroscopic grade. In some experiments the solvent was a 1:4 v/v water/methanol mixture. When necessary, the pH of these solutions was adjusted using diluted aqueous HCl or NaOH solutions, with the aid of a pH meter. The experimental absorption spectra were taken on a HACH DR-4000U spectrophotometer. The fluorescence measurements were done using a Hitachi F-4500 spectrofluorimeter equipped with low-temperature accessories. The fluorescence spectra were obtained, using right angle configuration, by exciting the sample at the wavelength of maximum excitation. The fluorescence quantum yields were estimated from the corrected fluorescence spectra using 9,10-diphenylanthracene in cyclohexane ($\Phi_{\mathrm{fl}} = 0.90$ at 20°C) as standard, using the methodology proposed by Eaton [5]. The solutions were prepared with absorbance at the excitation wavelength below 0.100.

---

* Corresponding author.

E-mail address: aeduardo@ufu.br (A.E. da Hora Machado).

1010-6030/01/$ – see front matter © 2001 Elsevier Science B.V. All rights reserved.
PII: S1010-6030(01)00461-0

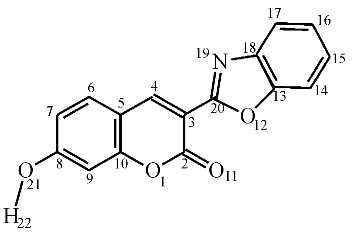

Fig. 1. Representation of the compound 3-benzoxazol-2-il-7-hydroxy-chromen-2-one with some atoms numbered.

Low-temperature measurements were made at 77 K, under liquid nitrogen, using methyl cyclohexane as solvent. The coumarin was previously dissolved with a little amount of 2-butanol, and the solutions were previously deoxygenated by bubbling argon.

Time resolved measurements were done on a CD-900 Edinburgh Analytical Instruments time resolved spectrophotometer, operating with a hydrogen filled nanosecond flash lamp at 30 kHz pulse frequency. All lifetime values reported reflect data taken with at least 1000 pulses in the maximum channel, and $0.900 < \chi^2 < 1.100$ during the measurements. The measurements were done, using the cuvette with the sample in a front-face configuration.

The quantum yield of singlet oxygen generation was measured in chloroform, using solutions with absorbance of 0.300 at 355 nm. The solvent was previously treated with activated silica for 12 h before its use in the measurements. The measurements were done, using an LP 900 Edinburgh Analytical Instruments time-resolved system, with 355 nm laser pulses (5 ns) furnished by a Nd-YAG Continuum Surelite II (Q-switched delay 200 μs). The laser power was varied from 0 to 8 mJ. A North Coast EO-817 detector was used for the detection of singlet oxygen phosphorescence at 1270 nm. Phenalenone ($\phi_{\Delta,\mathrm{s}} = 0.97$ at 20°C), Aldrich, was used as standard in these measurements, using the methodology proposed by Schmidt et al. [6] based on the following equation:

$$\phi_{\Delta,\mathrm{a}} = \frac{I_\mathrm{a}}{I_\mathrm{s}}\phi_{\Delta,\mathrm{s}}$$

where I_a is the emission intensity of the sample, I_s the emission intensity of the standard and $\phi_{\Delta,\mathrm{a}}$ the quantum efficiency of singlet oxygen generation by the sample. The excitation of the standard and samples was done at different laser powers. The ratio $I_\mathrm{a}/I_\mathrm{s}$ was calculated from the slopes of the plot signal intensity vs. laser power. The excitation of the standard (phenalenone) and samples was done at different laser powers. This permitted to do a more accurate evaluation of $I_\mathrm{a}/I_\mathrm{s}$. This value was obtained taking the ratio between the slope of the plot of the signal due to singlet oxygen at 1270 nm at $t = 0$ s expressed in millivolts, vs. the laser power, expressed in millijoules, for the sample and for the standard:

$$\frac{I_\mathrm{a}}{I_\mathrm{s}} \approx \frac{(\Delta S/\Delta P)_\mathrm{a}}{(\Delta S/\Delta P)_\mathrm{s}} = \frac{(\Delta S)_\mathrm{a}}{(\Delta S)_\mathrm{s}}$$

$(\Delta P)_\mathrm{a} = (\Delta P)_\mathrm{s}$, considering that the experiments were done under the same conditions.

The ground state geometries of the neutral and anionic forms were firstly optimized using the PM3 semi-empirical Hamiltonian (AMPAC 6.56 PC and Hyperchem 5.11 Pro). After, the geometries were refined using HF/STO-3G ab initio calculation (Gaussian 94W). With the new geometries, the prediction of the electronic spectra, microstates, oscillator strengths, dipole moments, bond orders and charges, was done using semi-empirical (PM3, Hyperchem 5.11 and AMPAC 6.56-PC, CI and SCF) single point calculations. For the prediction of the electronic spectra, 25 occupied and 25 unoccupied molecular orbitals were used in the CI calculations, totalizing 1251 configurations. In the theoretical spectrum, only the lines with oscillator strengths higher than 0.001 were represented. For microstate calculation, 400 configurations were used. The solvent role on the evaluated properties was also considered. In this case, the calculations were done using a variation of a Hyperchemistry option (Periodic Box), with a limited number of solvent molecules (methanol/water, approximately 20 molecules in each box, in a 1:1 ratio) in the neighbourhood, at a minimal distance of 2.3 Å between the solute and solvent atoms [7]. For the anionic form, the best representation reached for the solvation was an ionic pair (the anion and a H_3O^+) in a methanol/water mixture. In both cases, the initial conformation of the coumarin derivative was the one predicted by ab initio calculation. The set of molecules was firstly optimized before the single point calculations.

For a group of semi-empirical methods, the results obtained using PM3 showed, for this coumarin derivative, a better agreement with the experimental ones.

3. Results and discussion

3.1. Absorption spectra

In the range between 200 and 500 nm, the absorption spectrum for this coumarin presents, in a 1:4 v/v

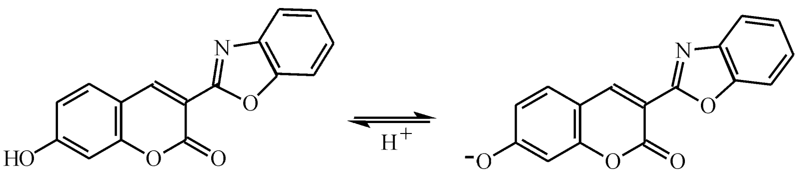

Scheme 1.

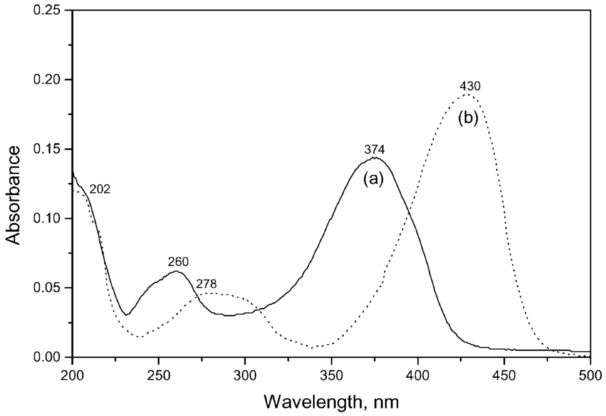

Fig. 2. Absorption spectra of: (a) neutral and (b) anionic forms in a 1:4 v/v water/methanol mixture.

water/methanol mixture, three typical absorption bands (202, 260 and 374 nm). The band centred at 374 nm due to $S_0 \rightarrow S_1$ transition, is attributed mainly to $\pi \rightarrow \pi^*$ transition, considering its high molar absorptivity, around 10^4 dm^3 mol^{-1} cm^{-1}, and also the results of quantum mechanical calculation. Also, the fluorescence lifetime, between 2.5 and 5.2 ns, observed for solvents of different polarities (Table 4) reinforces this [8]. For the anionic form, the absorption bands occurs at 202, 278 and 430 nm, in the same solvent mixture. The displacement of the $S_0 \rightarrow S_1$ band is attributed to the dissociation of the phenolic hydroxyl group, which increases the electronic delocalization in the structure. The first and second bands should be attributed, respectively, to ethylenic, and benzenoid transition for both forms [9]. The molar absorptivity corresponding to the $S_0 \rightarrow S_1$ transition, for the anionic form, possesses the same magnitude verified for the neutral form. Fig. 2 shows the superimposed spectra for both forms.

The data for the $S_0 \rightarrow S_1$ transitions, estimated by semi-empirical calculations show a good agreement with the experimental ones, for both species (see Table 1), principally when the calculations are done considering the solvation of the species.

The electronic spectra for both forms reproduce well the position of the experimental maxima even considering the species being isolated. The absorption maxima corresponding to the $S_0 \rightarrow S_1$ transition for the anionic form displaced from 466.7 (isolated ion) to 409.3 nm, when in the calculation the solvent and a counter-ion (H_3O^+) were included. The discrepancy between experimental and theoretical data is of −7.9% for the isolated anion, and +5.1% for the solvated form. For the neutral molecule, the absorption maxima changed from 370.8 to 386.9 nm with, respectively, +0.9 and −3.4% of discrepancy, from the isolated to the solvated form. The inclusion of the solvent also results in a better description of the spectra in all the range of the experimental spectra. Some spurious lines observed in the absorption spectra of the isolated molecules disappeared when solvent molecules were included in the calculation (see Fig. 3).

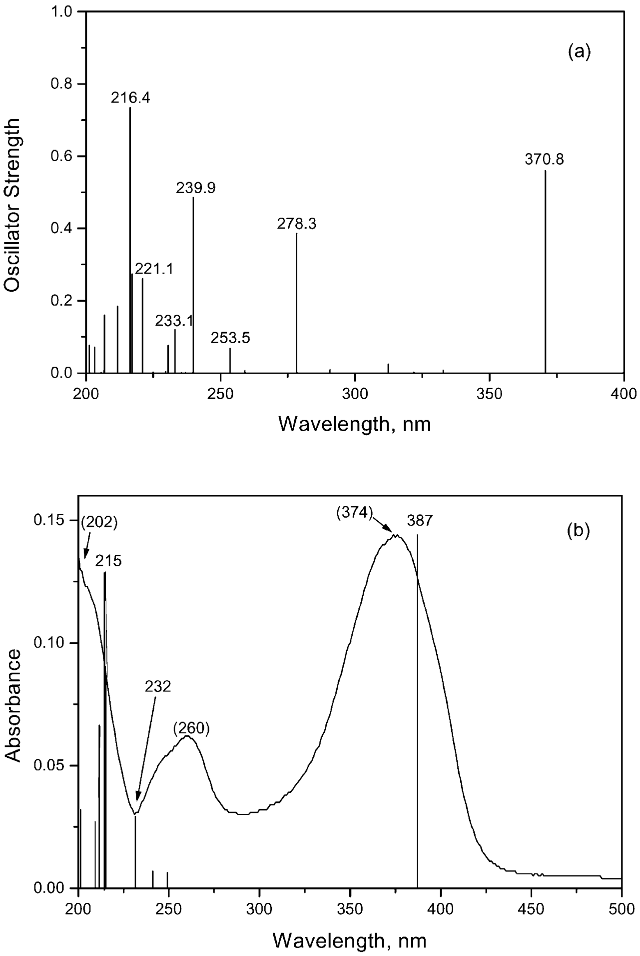

Fig. 3. Calculated absorption spectra (PM3 CI): (a) neutral form, isolated; (b) neutral form, solvated (methanol/water) in superposition with the experimental spectrum in a 1:4 v/v water/methanol mixture.

Table 1
Absorption maxima ($S_0(v = 0) \rightarrow S_1(v = n)$), oscillator strength and molar absorptivities, for solutions prepared in 1:4 v/v water/methanol mixtures

Coumarin	λ_{max} (PM3) (nm)	f (PM3)	λ_{max} (experimental)[b] (nm)	f (calculated)[c]	log ε
Neutral, isolated	370.8	0.5604	–	–	
Neutral, solvated[a]	386.9	0.8566	374	0.3537	4.410
Ionized, isolated	466.7	1.0796	–	–	–
Solvated, ionic pair[a]	409.3	0.9506	430	0.3423	4.528

[a] PM3 water/methanol.

[b] From experimental absorption spectra.

[c] f (calculated) $= 4.319 \times 10^{-9} \int \varepsilon(\bar{v})\mathrm{d}\bar{v}$, where $\int \varepsilon(\bar{v})\mathrm{d}\bar{v}$ is the area under a curve of the molar extinction coefficient plotted against wavenumber.

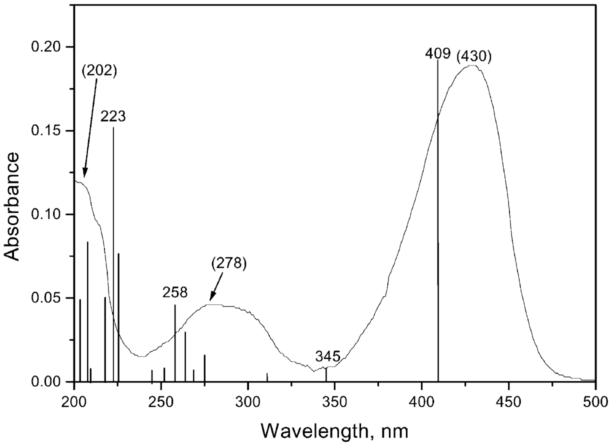

Fig. 4. Theoretical electronic spectrum for the anionic form, solvated, ionic pair, superimposed with the experimental spectrum taken using a 1:4 v/v water/methanol mixture as a solvent at pH 10.54. The theoretical points were normalized from the experimental curve.

Fig. 4 shows the experimental and theoretical spectra for the anionic form, with the corresponding theoretical spectrum obtained for the solvated molecule. The oscillator strength (Table 1) estimated by theoretical calculation, unless the extremely high values agree with the expected for the character of the $S_0 \rightarrow S_1$ transition, which presents an elevated molar absorptivity.

3.2. Microstates

The prediction of the microstates for the neutral form is improved when the influence of the solvent is considered in the calculations, showing the inclusive of the expected effects related to the solvent relaxation. This can be deduced by the comparison of the S_1 state energy calculated and experimentally obtained. For the neutral and anionic forms, the experimental S_1 energies were estimated as being, respectively, 286.08 and 257.91 kJ/mol. The calculated value for the neutral form, isolated, is 365.92 kJ/mol (Table 2). Considering the solvation, the value for S_1 energy decreases to 321.11 kJ/mol. This indicates that a suitable consideration of the solvation in the calculations tends to approach the theoretical result to the experimental one. Most probably, the increase in the number of configurations with a good description of the solvation environment must result in a safe description of the electronic structure of the molecule.

For the anionic form, isolated, the calculated S_1 energy is 270.20 kJ/mol. This value for the solvated species suffers an increase to 310.78 kJ/mol. This could be seen as an indication of the lack of stability for this species when solvated, which is not true. On the other hand, this model gave a good description of the electronic spectrum of the solvated anionic species. It is evident that it needs to be improved to furnish a best description of the electronic structure and correlated properties for the solvated anionic species.

For both species, the calculated electronic structure shows a series of electronic states in close proximity to the S_1 state (Fig. 5). A similar observation was done by McCarthy and Blanchard [10] in a study of the electronic structure of several coumarins involving molecular orbital calculations based on the AM1 Hamiltonian.

The calculated electronic structure of this coumarin shows a reasonable complexity. For the neutral form, solvated, at least two triplet states occur with energies lower than the S_1 energy. The energy difference between S_1 and T_2 is equal to 0.21 kJ/mol, a very little value which justifies elevated values for the quantum yield of intersystem crossing, in disagreement with the experimental data: phosphorescence was not detected in our experiments at 77 K, the fluorescence quantum yield shows to be high for solvents with different polarities, and a very small quantum yield of singlet oxygen generation ($\Phi_\Delta = 0.06$) was measured using chloroform as solvent. However, for another class of coumarins, we have obtained a theoretical description of their electronic structure in close agreement with the experimental ones [14].

The calculated dipole moment for the neutral and anionic species show that while this parameter increases from S_0 to S_1 for the neutral form, it decreases for the anionic form (Table 2). The lower dipole moment for the S_1 state implies in a lower probability of solvent relaxation for the anionic species, as the polarity increases, when compared with the neutral one. Also, the results of theoretical calculation show that the anionic species must present a higher rigidity than the neutral, reducing the chances of vibrational relaxation of the S_1 sate of the anionic species when solvated. The formation of ionic pairs between the anionic species and its counter-ion must to potentialize the internal conversion as non-radiative deactivation pathway (Table 4).

Table 2
Dipole moments for the coumarin, and geometric parameters (bond length, BL, dihedral angle, D, and bond order, BO) between the benzoxazol and chromen-2-one groups, calculated using ab initio and semi-empirical calculations

Form	S_0				S_1			
	μ^a (D)	BL^a (Å)	D^a (°)	BO^b	μ (D)	BL (Å)	D (°)	BO
Neutral	1.499	1.487	0.056	0.997	1.812	1.489	0.017	1.152
Anionic	9.374	1.446	0.048	1.105	8.590	1.426	0.006	1.221

[a] Ab initio calculation.

[b] Single point semi-empirical calculation.

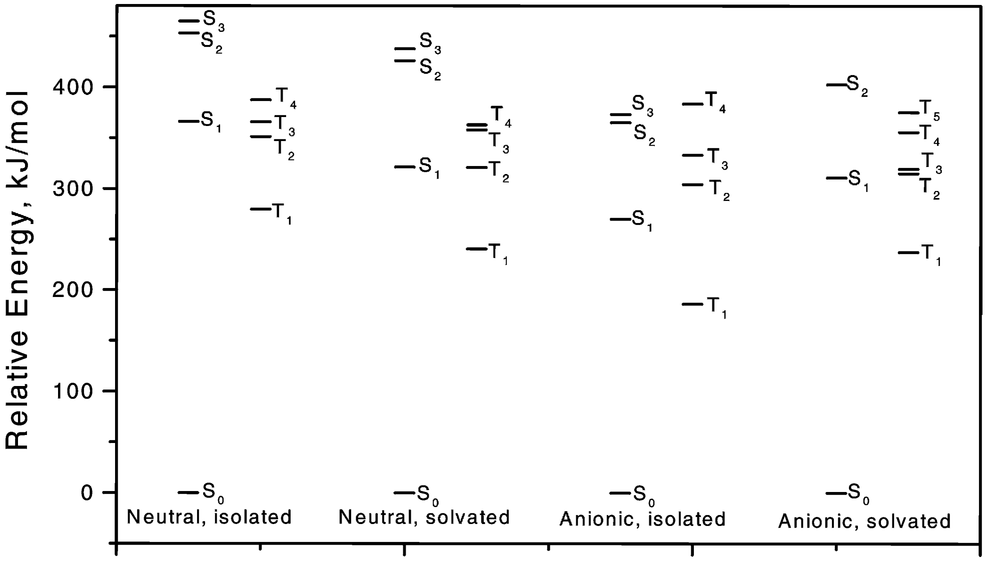

Fig. 5. PM3 CI electronic excited states for the neutral and anionic forms. The solvation was simulated considering a mixture of an equal number of molecules of water and methanol as solvent.

The calculations made for the isolated molecule, indicate a perturbational contribution of $n \rightarrow \pi^*$ transition for the S_1 state of the anionic form due to the contribution of the phenoxide group, which explains the decrease in the dipole moment (see Table 2). For the neutral form, the ketonic group also contributes with an $n \rightarrow \pi^*$ perturbational component, although in this case this contribution does not results in significant changes in the pattern of the $\pi \rightarrow \pi^*$ transition. The analysis of the changes occurred on the atomic charges and bond orders for both species at the S_0 and S_1 states (see Fig. 1 and Table 3) supports this. For the neutral species, a charge transfer from the oxygen (O_{11}) to the carbon (C_2) in the carbonyl group can be verified, considering the variation from −0.547 to −0.474 in the difference of the net charges over these atoms, Δq (−13.3%), occurred simultaneously by a reduction of −9.6% in the bond order of this bond, from 1.875 to 1.695. These variations in the ketonic group are negligible for the anionic species. On the other hand, for this species, Δq varied −8.2%, from −0.499 to −0.458, and the bond order −10.1%, from 1.747 to 1.570, for the bond between the atoms O_{21} and C_8, denoting a charge transfer from O_{21} to the chromen-2-one ring, which is not observed for the neutral form.

3.3. pk_a measurement

Fig. 6 shows the behaviour of identical solutions in a 1:4 v/v water/methanol mixture at different pH's.

The dissociation equilibrium for this compound was evaluated considering the bathochromic displacement of the $\mathrm{S}_0 \rightarrow \mathrm{S}_1$ band, due to the increase of pH. The pk_a, estimated directly from the curve A_{430} vs. pH for methanol/water solutions is 6.33 ± 0.03.

As pH increases, a shoulder evidencing the deprotonation of the coumarin appears at 430 nm. This is more evident when these spectra are taken under different solvents, like as pure methanol and DMF. Fig. 7 shows the superposition of the spectra taken under these conditions. In methanol the preponderant form is the neutral with a maximum at 380 nm. A shoulder at 466 nm can also be seen. This shoulder, due to the presence of the molecules in the anionic form, is viewed as a peak DMF, in which the deprotonation of

Table 3
Bond orders (BO) and charges (q) for the S_0 and S_1 states of the neutral and anionic forms of the compound 3-benzoxazol-2-il-7-hydroxy-chromen-2-one

Atom	Neutral					Anionic			
	S_0			S_1		S_0		S_1	
	q^{a}	Bond	BO^{b}	q^{a}	BO^{b}	q^{a}	BO^{b}	q^{a}	BO^{b}
C_2	+0.313	$\mathrm{C}_2\mathrm{O}_1$	0.953	+0.256	0.976	+0.294	0.956	+0.291	0.959
C_8	+0.146	$\mathrm{C}_8\mathrm{C}_7$	1.293	+0.145	1.223	+0.168	0.992	+0.134	1.082
O_{11}	−0.234	$\mathrm{O}_{11}\mathrm{C}_2$	1.875	−0.218	1.695	−0.309	1.776	−0.309	1.799
O_{21}	−0.269	$\mathrm{O}_{21}\mathrm{C}_8$	1.066	−0.268	1.086	−0.331	1.747	−0.324	1.570

[a] Ab initio calculation.
[b] AMPAC 6.56 PC PM3.

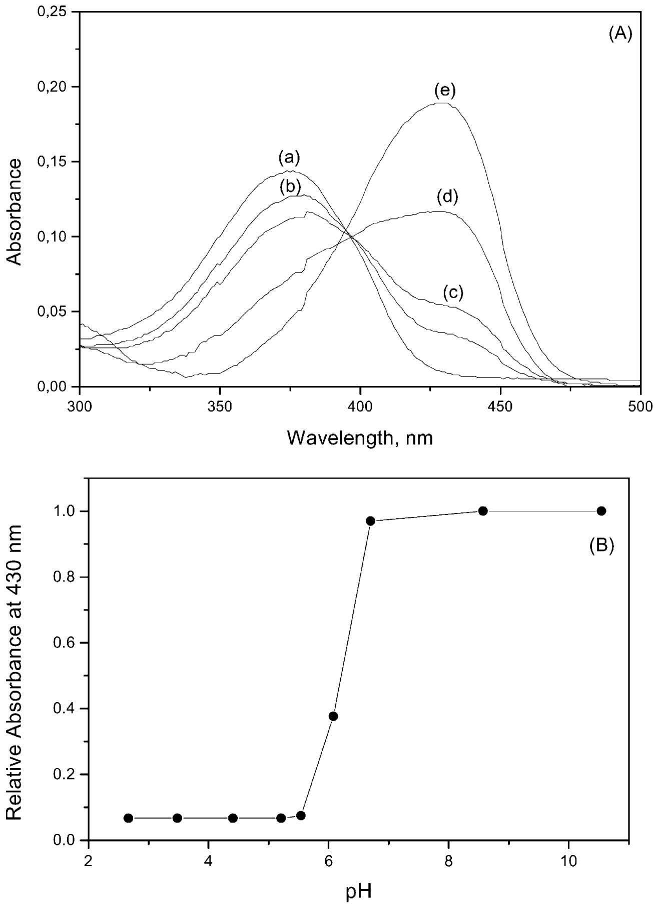

Fig. 6. (A) Absorption spectra of 3-benzoxazol-2-il-7-hydroxy-chromen-2-one as a function of pH: (a) pH 2.67; (b) pH 5.54; (c) pH 6.08; (d) pH 6.70; (e) pH 10.54. (B) Sigmoidal curve for the pk_a determination. Solvent: 1:4 v/v water/methanol.

the hydroxyl group occurs efficiently. Methanol, due to its capability to promote the formation of hydrogen bonds will favour in a minor extent the displacement of the dissociation equilibrium (Scheme 1).

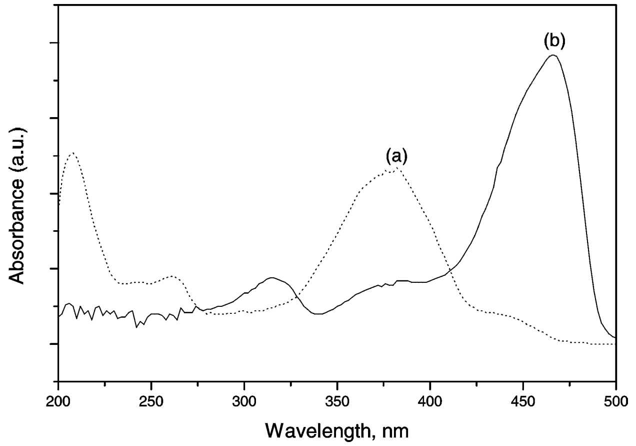

Fig. 7. Absorption spectra of the compound 3-benzoxazol-2-il-7-hydroxy-chromen-2-one in methanol (a) and dimethylformamide (b).

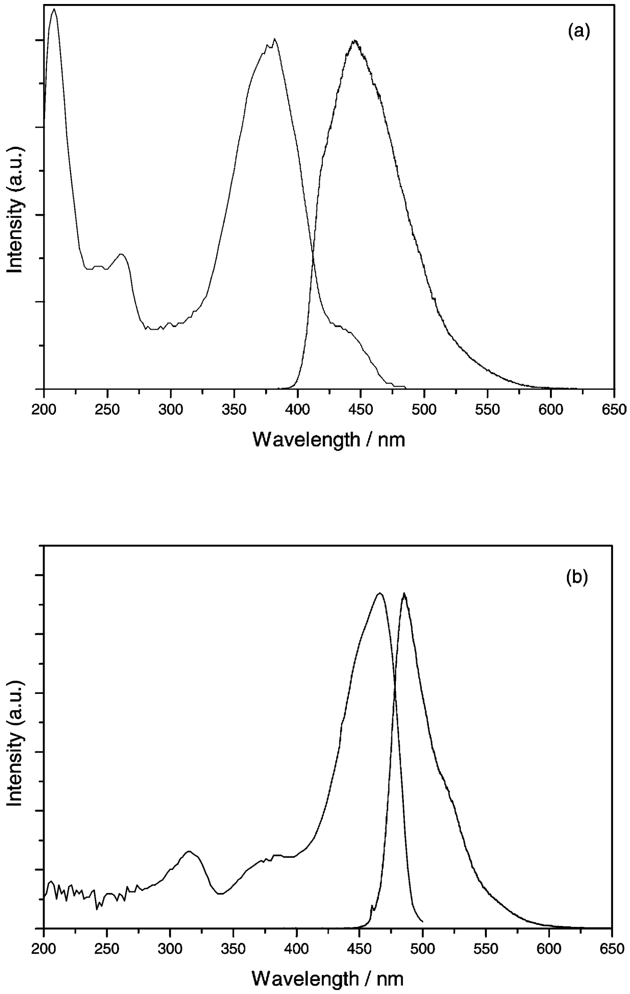

Fig. 8. Absorption and emission spectra for the coumarin derivative in: (a) methanol and (b) dimethylformamide (DMF).

3.4. Fluorescence

As shown in Fig. 8, the fluorescence spectra for both forms are approximately the specular image of the absorption spectra. This trend occurs for the different solvents studied. This behaviour can be seen as an indication that the geometry of the S_1 state is nearly similar than that of S_0 state [11,12], which confirms the theoretical results.

These results do not show substantial geometry changes for the S_1 state for both species, when compared with the ground state, unless a higher structural rigidity for the anionic form, and changes in the length of the molecule, reflected by the values of dipole moment. For the neutral molecule, the angle between rings changed from 0.049° to 0.017° with its excitation. The highest planarity of the excited state can be followed by the comparison of the bond orders for the bond $C_{20}C_3$, between the rings (Table 2). An increase of 15.5% is verified for the neutral species, and must be the result of a redistribution of the π electronic cloud over the molecule. For the anionic form, the

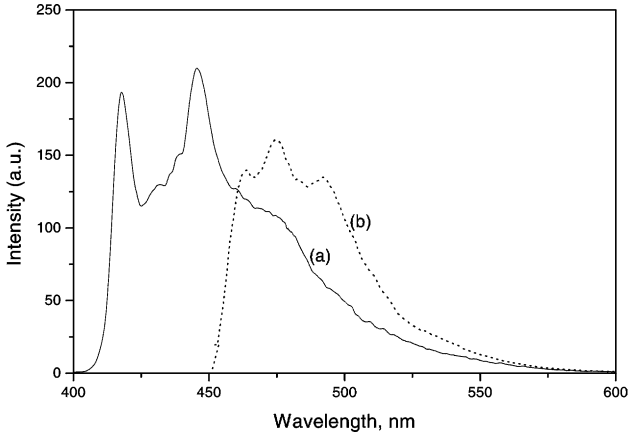

Fig. 9. Fluorescence spectra for the coumarin derivative at 77 K: (a) neutral form, $S_1 = 286.08$ kJ/mol; (b) anionic form, $S_1 = 257.91$ kJ/mol. Solvent: methyl cyclohexane.

structure in the ground state presents a torsion angle of 0.038° between the rings, while for the S_1 excited state is 0.006°. Also, an increase in the delocalization of the π electronic cloud with the excitation must be expected: the bond order of the $C_{20}C_3$ bond suffered an increase of 10.5%.

Fig. 9 shows the superposition of the fluorescence spectra for the neutral and anionic forms of this compound at 77 K. Both spectra show a good structuration, which permitted a safe estimative of S_1 energy.

As can be seen from Table 4, the fluorescence quantum yields are usually high for both forms. This occurs due to the presence of the hydroxyl group in position 7, and the benzoxazolyl group in position 3, of the chromen-2-one ring [4,13]. The estimated mean value of fluorescence quantum yield for the neutral form is 0.87 at 298 K for the solutions prepared in a 1:4 v/v water/methanol mixture, and 0.94 at 77 and 298 K, in methyl cyclohexane. For the anionic form, these values are usually lower: 0.53 at 298 K for the solutions prepared in a 1:4 v/v water/methanol mixture, and 0.79 and 0.63, in methyl cyclohexane, respectively, at 77 and 298 K.

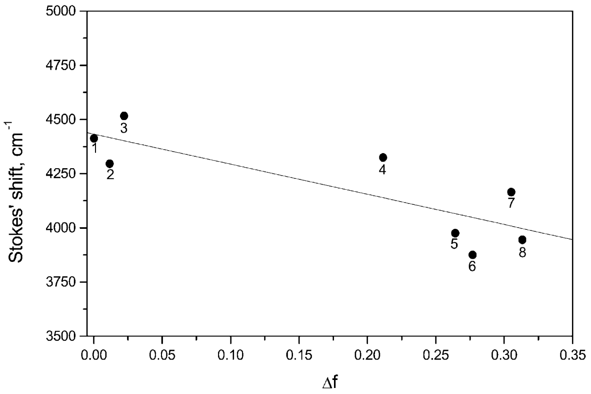

Fig. 10. Lippert relationship for the coumarin derivative for different solvents: methyl cyclohexane (1), carbon tetrachloride (2), 1,4-dioxane (3), tetrahydrofuran (4), 2-butanol (5), isopropanol (6), acetonitrile (7), methanol (8).

Considering the polarity parameter known as orientation polarizability, Δf, we can see that Φ_f does not show any significative change at 298 K unless for DMF and ethylene glycol. For the first, $\Phi_f = 0.57$, this trend agrees with that observed for water/methanol solutions at alkaline pH, where the ionic pairs between the anionic species and its counter ion must potentialize the internal conversion as non-radiative deactivation route. For ethylene glycol, $\Phi_f = 0.77$, despite its high viscosity. This low value for Φ_f is most probably associated to the ability of this solvent to form hydrogen bonds with the coumarin, potentializing the non-radiative route for the deactivation of the S_1 excited state.

As can be seen by the ratio k_f/k_{nr}, as the polarity increases the non-radiative process become more pronounced. For example, for carbon tetrachloride with $\Delta f = 0.012$, where no significant polar interaction between the S_1 state and the solvent is expected, this ratio is 128.67, whereas for ethylene glycol with $\Delta f = 0.276$, $k_f/k_{nr} = 3.34$. In general, can be concluded that the deactivation of the S_1 state is preponderantly fluorescent. Although, some intersystem crossing

Table 4
Photophysical parameters for the compound 3-benzoxazol-2-il-7-hydroxy-chromen-2-one in different solvents

Solvent	Δf^{a}	λ_{max} (nm)	log ε	λ_{exc} (nm)	λ_{em} (nm)	Φ_f	ΔStokes (cm^{-1})	τ_{exp} (ns)	τ_f (ns)	$k_{exp} \times 10^{-8}$ (s^{-1})	$k_f \times 10^{-8}$ (s^{-1})	$k_{nr} \times 10^{-8}$ (s^{-1})
Methyl cyclohexane	0.000	381	–	381	458	0.94	4413	–	–	–	–	–
Carbon tetrachloride	0.012	382	4.38	387	457	0.99	4296	2.569	2.59	3.89	3.86	0.03
1,4-Dioxane	0.022	374	4.34	372	450	0.93	4516	–	–	–	–	–
Tetrahydrofuran	0.212	376	4.43	375	449	0.82	4324	–	–	–	–	–
2-Butanol	0.264	381	4.38	381	449	0.99	3975	–	–	–	–	–
Dimethylformamide	0.276	466	4.62	468	485	0.57	841	2.579	4.52	3.88	2.21	1.67
Ethylene glycol	0.276	382	4.38	382	451	0.77	4001	2.452	3.18	4.08	3.14	0.94
Isopropanol	0.277	381	4.41	381	447	0.97	3875	–	–	–	–	–
Acetonitrile	0.305	374	4.33	371	443	0.98	4165	–	–	–	–	–
Methanol	0.313	380	4.41	381	447	0.94	3944	–	–	–	–	–
CH_3OH/H_2O 4:1, pH 2.67	–	374	4.41	374	468	0.68	5364	2.768	4.07	3.61	2.46	1.15
CH_3OH/H_2O 4:1, pH 5.21	–	374	4.38	374	464	0.87	5044	2.856	3.28	3.50	3.05	0.45
CH_3OH/H_2O 4:1, pH 10.54	–	430	4.53	430	469	0.53	1934	2.742	5.13	3.65	1.95	1.70

[a] Orientation polarizability.

must occur, despite the absence of detectable phosphorescence at 77 K. A very small quantum yield of singlet oxygen generation ($\Phi_\Delta = 0.06$) was measured for this coumarin in chloroform (Fig. 10).

On the other hand, when the relation between the Stokes' shift and Δf is analysed, an apparently unexpected behaviour is found. The next figure shows an inverse linear relation between these two parameters. This behaviour can be understood if we consider the occurrence of increasing specific solvent–fluorophore interactions in the ground state as the polarity increases, which can be seen by the red shift observed for the absorption maxima [11]. Despite of the increase of the dipole moment, verified when the neutral species is in the S_1 state, these specific solvent–fluorophore interactions become practically unchanged between both states to justify a large variation than the observed for the Stokes' shift with the polarity. Excluding the solvents methyl cyclohexane and carbon tetrachloride, all the other solvents possess high dielectric constants and different hydrogen bonding ability, parameters which must be decisive for the mentioned interactions. However, DMF was not included in this series, due to its observed high capability to deprotonate the compound under study. For this solvent, the effect of the solvent–fluorophore interactions is more pronounced despite the value of Δf (Table 4). These interactions must affect directly the routes of deactivation of the excited state, increasing the participation of internal conversion.

Acknowledgements

To CNPq, CAPES and FAPEMIG for research grants. To Maria C. Bartasson, undergraduate student, Dr. Maurício S. Matos and Dr. Reinaldo Ruggiero for their collaboration in some experiments and valuable discussions, to Dr. Ana Maria F. de Oliveira-Campos, University of Minho, Portugal. To LERT/IQ/UFRJ (Professors David E. Nicodem and Ira Mark Brinn) and Laboratório de Fotoquímica/IQSC/USP (Professors Miguel Guillermo Neumann and Marcelo Gehlen) for the cession of their laboratorial infrastructures.

References

[1] B.M. Krasovitskii, in: B.M. Krasovitskii, B.M. Bolotin (Eds.), Organic Luminescent Materials, VCH, Weinheim, 1988 (Chapter 7).
[2] K.H. Drexhage, in: F.P. Schäfer (Ed.), Topics in Applied Physics, Vol. 1, Dye Lasers, Springer, Berlin, 1973.
[3] C.E. Wheelock, J. Am. Chem. Soc. 81 (1959) 1348.
[4] J.S. Seixas de Melo, R.S. Becker, A.L. Maçanita, J. Phys. Chem. 98 (1994) 6054.
[5] D.F. Eaton, Pure Appl. Chem. 60 (1988) 1107.
[6] R. Schmidt, C. Tanielian, R. Dunsbach, C. Wolff, J. Photochem. Photobiol. A 79 (1994) 11.
[7] Hyperchemistry 5.11 Manual, Hypercube, 1999.
[8] R.S. Becker, Theory and Interpretation of Fluorescence and Phosphorescence, Wiley/Interscience, New York, 1969.
[9] R.M. Silverstein, G. Clayton Bassler, T.C. Morrill, Spectrometric Identification of Organic Compounds, 5th Edition, Wiley, Singapore, 1991.
[10] P.K. McCarthy, G.J. Blanchard, J. Phys. Chem. 97 (1993) 12205.
[11] J.R. Lakowicz, Principles of Fluorescence Spectroscopy, Kluwer Academic Publishers/Plenum Press, New York, 1999.
[12] N.J. Turro, Modern Molecular Photochemistry, University Science Books, California, 1991.
[13] R.M. Christie, C.-H. Lui, Dyes and Pigments 42 (1999) 85.
[14] A.E. da Hora Machado, J.A. de Miranda, A.M.F. de Oliveira-Campos, Unpublished results.